

Using the Weather Research and Forecasting (WRF) Model to Predict Ground/Structural Icing

Gregory Thompson,^{*} Bjorn Egil Nygaard,[†] Lasse Makkonen,[‡] and Silke Dierer[#]

^{*}National Center for Atmospheric Research, Boulder, CO, USA (gthompsn@ucar.edu)

[†]Norwegian Meteorological Institute

[‡]Finnish Meteorological Institute

[#]MeteoTest

Abstract—A new cloud/precipitation physics module was developed for the Weather Research and Forecasting and other mesoscale models. The scheme explicitly predicts the mass of cloud water, cloud ice, rain, snow, and graupel and has been adapted to the problem of forecasting aircraft icing using the direct output of predicted supercooled water. Likewise, the scheme can be readily applied to the problem of ground/structural icing because the median volume diameter of the supercooled water can be easily calculated for use in ice accretion models. Since the model includes all of the fundamental physics of precipitation, it can predict mixed phase conditions, freezing drizzle and rain, and wet snow as well as riming due solely to small cloud droplets (freezing fog). In this paper, preliminary results of high-resolution WRF simulations of ground/structural icing events will be discussed. Various methods to calculate severity of icing conditions on ground structures will be presented and compared to icing observations at the surface. One of the case studies is a multiple-day icing event on a TV tower in Helsinki, Finland. Accurate prediction of ground/structural icing remains a difficult challenge, due to model deficiencies in representing many physical processes: radiation, boundary layer and turbulent exchange as well as microphysics.

I. NOMENCLATURE

GFS — Global Forecast System
 LWC — liquid water content
 MVD — median volume diameter
 SLW — supercooled liquid water
 USGS — United State Geological Survey
 WRF — Weather Research and Forecasting model

II. INTRODUCTION

Explicit prediction of ground/structural icing requires knowledge of the ambient temperature, wind speed, and size and number of water drops and ice crystals impinging on the surface object. Over the past few decades, computer models have clearly improved predictions of temperature and wind, though, in general, predictions at middle and high altitudes are more accurate than predictions nearest the ground where far more variability in local conditions exist. Nonetheless, near-surface forecasts of wind and temperature have improved to some degree as well as explicit forecasts of precipitation type and amount. Future improvements in surface precipitation forecasts are expected since model numerics and physics are constantly improved and computer power increases allowing both higher resolution simulations and more complex physical processes to be modeled.

One effort in the past few years towards more accurate precipitation forecasts includes the development of a new cloud/precipitation physics parameterization for mesoscale weather prediction models. The scheme is extensively described in Thompson et al, 2008 and is available within the Weather Research and Forecasting (WRF) model (Skamarock et al, 2008), which can be readily found and downloaded from the internet. In developing the new cloud/precipitation physics scheme, also called a bulk microphysical parameterization, a primary goal was to improve explicit forecasts of supercooled liquid water. More specifically, the original objective was to improve forecasts of aircraft icing aloft, but the problem of ground/structural icing is very similar and the scheme is well-suited for applying to ground icing as will be shown in this paper.

The new scheme explicitly predicts the mass of cloud water, cloud ice, rain, snow, and graupel. In addition, the number concentrations of cloud ice and rain are explicitly predicted, while the number of snow and graupel are diagnosed from various assumptions and the number of cloud droplets is currently set constant. A future version of the scheme will contain explicit prediction of cloud droplet number based on available condensation nuclei. Along with liquid water content (LWC), number of cloud droplets, and assumptions of how the mass is distributed with respect to size, the median volume diameter (MVD) can be computed diagnostically, which strongly influences the accretion of rime ice on surface structures. The next section describes the procedure to compute MVD from model output and apply it to the problem of estimating ice accretion. In the subsequent section, the mesoscale model configuration is discussed followed by a section with details of numerous case studies that were investigated.

III. ESTIMATING ICE ACCRETION FROM MODEL OUTPUT

A. Diagnosing MVD of Cloud Droplets

In its current form, the microphysics scheme utilizes a constant number of cloud droplets that should be set according to general characteristics of the simulated environment, as in, maritime or continental aerosol concentration. Many simulations will include regions with both environments, but the scheme is currently designed for a single value of cloud droplet concentration at all grid points for the duration of the simulation. A moderate sensitivity exists between droplet concentration and median volume diameter, however, since there exists

no routine observations of number concentration, it is extremely difficult to model accurately its evolution in most cloud simulations. During some research field projects, measurements of droplet number are available and many of these events were investigated while developing the microphysics scheme.

As described in full detail in Thompson et al, 2008, cloud water is assumed to follow a generalized gamma distribution of the form:

$$N(D) = N_0 D^\mu e^{-\lambda D} \quad (1)$$

where $N(D)$ is the number of droplets of a specified diameter, D , N_0 is the intercept parameter, λ is the slope of the distribution, and μ is the shape parameter, diagnosed from the pre-specified droplet number, N_c (in per cubic centimeter), using:

$$\mu = \min(1000/N_c + 2, 15) \quad (2)$$

Then, to diagnose MVD of cloud droplets, we use the value of μ in combination with the model output LWC using:

$$MVD = (3.672 + \mu)/\lambda \quad (3)$$

where λ is defined from integrating (1) over all diameters with the mass of spherical water drops resulting in:

$$\lambda = \left[\frac{\pi}{6} \rho_w \frac{\Gamma(4 + \mu)}{\Gamma(1 + \mu)} \left(\frac{N_c}{LWC} \right) \right]^{1/3} \quad (4)$$

B. Computing the Ice Accretion

The computed MVD can then be used in calculating a collection efficiency for the ice accretion equation of Makkonen, 2000, which also contains the model output variables of wind speed, and LWC. More specifically, the growth rate of icing, dM/dt , is given by:

$$\frac{dM}{dt} = \alpha_1 \alpha_2 \alpha_3 LWC v A \quad (5)$$

where A is the cross-sectional area of the object (relative to the direction of the particle velocity vector, v) and correction factors α_1 , α_2 , and α_3 denote the collision, sticking, and accretion efficiencies respectively.

In most applications when considering cloud droplets, the latter two factors are essentially unity, because nearly every droplet that hits the object will stick and the small size of cloud droplets entirely freeze and they do not run off the surface. However the collision efficiency for small drops is less than unity since they can be carried by the airflow around the object due to their small inertia. Larger drops of drizzle or rain, however, have enough inertia such that these drops will hit the surface producing a collision efficiency of one but may have lower than unity accretion efficiency since the largest drops may not entirely freeze before some water drips off the surface object on the ground below. The sticking efficiency, α_2 , is lower than unity only when ice/snow particles bounce off the surface object, which is more likely during conditions that are well below melting temperature and are not liquid coated. Makkonen (2000) provides advice for calculating all of the efficiencies when considering riming or glaze icing or wet snow accretion.

Returning to the problem of computing a collision efficiency of small cloud droplets, the equations reported in Makkonen are used :

$$\alpha_1 = A - 0.028 - C(B - 0.0454), \quad (6)$$

where

$$\begin{aligned} A &= 1.066K^{-0.00616} \exp(-1.103K^{-0.688}), \\ B &= 3.641K^{-0.498} \exp(-1.497K^{-0.694}), \\ C &= 0.00637(\phi - 100)^{0.381} \end{aligned} \quad (7)$$

and dimensionless parameters, K and ϕ are computed from:

$$K = \rho_w MVD^2 / 9\mu D, \quad (8)$$

and

$$\phi = Re^2 / K, \quad (9)$$

where D is the cylinder diameter and the droplet Reynolds number, Re , based on the free stream velocity, v , is given by

$$Re = \rho_a MVD v / \mu, \quad (10)$$

with density and viscosity of air, ρ_a , and μ respectively.

IV. MESOSCALE MODEL SET-UP

For each of the case studies in the next section, the WRF model was configured with two nested grids, the outer one with 9 km grid spacing and the inner grid with 3 km spacing. Model forecasts varied in length depending on the event but ranged from 36 to 48 hours for most cases, except one case that was simulated for ten days in order to match the approximate duration of the entire event. The WRF model was initialized using analyses from the Global Forecast System (GFS) model with a grid point every half-degree latitude and longitude. The model domains were sufficiently large to minimize the forcing effects from the lateral boundary conditions, which were also supplied by the GFS analyses at 6-hourly intervals. The inner grid's terrain was generated from high-resolution USGS 30-second topography data. Fig. 1 shows a plot of the typical



Fig. 1. Plot of WRF model grids used for simulating the Guetsch, Switzerland event discussed in section V—B.

grid configurations for one of the cases presented in the next section. Each case had similar size domains centered on the area of interest.

V. CASE STUDIES

A variety of case studies were simulated with the WRF model including events of rime icing from cloud droplets, glaze icing from freezing rain or freezing drizzle, and wet snow. Not all of the case studies can be detailed within this document, but some representative results from a number of cases are included below.

A. Helsinki, Finland, 9-19 January 1996

During an especially prolonged rime icing event in Helsinki, most residents were unaware that anything strange was underway, until they lost TV reception. It is not unusual to have a long duration of cloudy weather with periods of rain or snow in January in Helsinki, but 1996 rarely had clear skies yet set a record for least precipitation (4.6 mm). For one of those weeks, a low cloud persisted over southern Finland with super-cooled cloud droplets collecting and freezing on structures that penetrated into the base of the cloud. Two such structures were TV broadcast antenna: the Pasila TV Centre tower is 117 m tall near the center of Helsinki, and the Kivenlahti TV tower, west of Helsinki, is 328 m tall and was often obscured by the cloud. A photograph of the icing accumulation taken near the end of the event is shown in Fig. 2.



Fig. 2. Photograph of icing accumulated on Kivenlahti TV tower (courtesy of A. Photographer).

From meteorological data collected at the Kivenlahti tower site, the icing begins to accrete during the second half of 11 Jan and persisted for nearly a week. Corresponding observations from the Vantaan airport in Helsinki frequently showed the cloud base lower than 200 m above ground during the same week. A time-series plot of temperature and wind data from Kivenlahti is shown in Fig. 3.

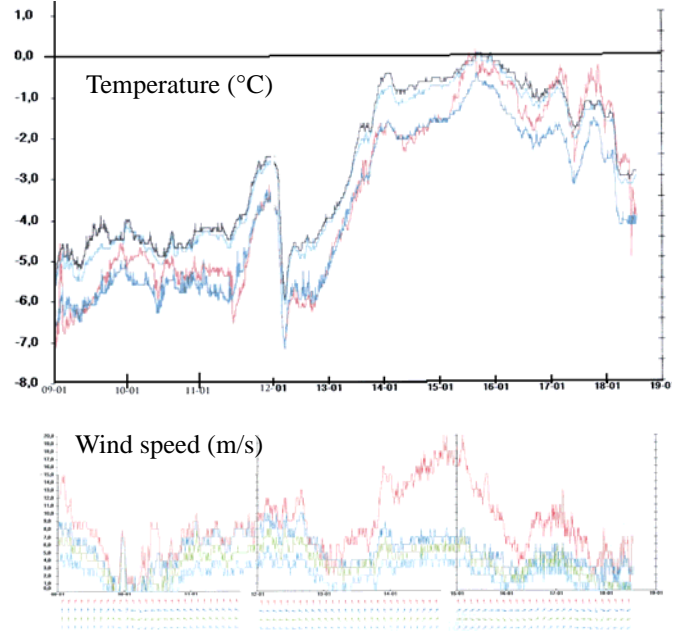


Fig. 3. Time-series of temperature ($^{\circ}\text{C}$; upper panel) and wind speed (m/s; lower panel) from the Kivenlahti TV tower. Sensors are located at 2 m (black line), 26 m (light blue), 91 m (green), 186 m (dark blue), and 298 m (red).

In general, when the near-surface winds included a component from the east, then the temperature would decrease whereas a southerly wind would produce a slight warming trend and, most likely, include more moisture, lower cloud base, and the most ice accretion. Few, if any, observers on the ground knew the tower was accumulating large ice loads until the TV signal was impeded by the ice coating. The first observations of ice were collected at 1200 UTC 17 Jan at the Pasila TV tower and the next morning at 0800 UTC at the Kivenlahti site. Therefore, very little is known about the time evolution of the ice accretion.

In an effort to make the most realistic simulation of this event, the WRF model was configured with a third grid with 1 km spacing in the region of the two TV towers. The simulation began at 0000 UTC 09 Jan and ran through 0000 UTC 19 Jan, ending after the first Kivenlahti tower observation. Overall, the WRF simulation produced a very long-lived and low cloud sometimes contacting the ground. Many model variables are shown in Fig. 4 for comparison with the observations shown in Fig. 3. One major discrepancy with the model simulation is the slightly too high model temperature forecast during the maximum observed on 15-16 Jan. The model forecasted 1.0 to 1.5 $^{\circ}\text{C}$, whereas the maximum in the observations remained at or below 0 $^{\circ}\text{C}$. This relatively minor error obviously directly impacts any calculations of ice load since ice would not accumulate when temperature exceeds 0 $^{\circ}\text{C}$. For

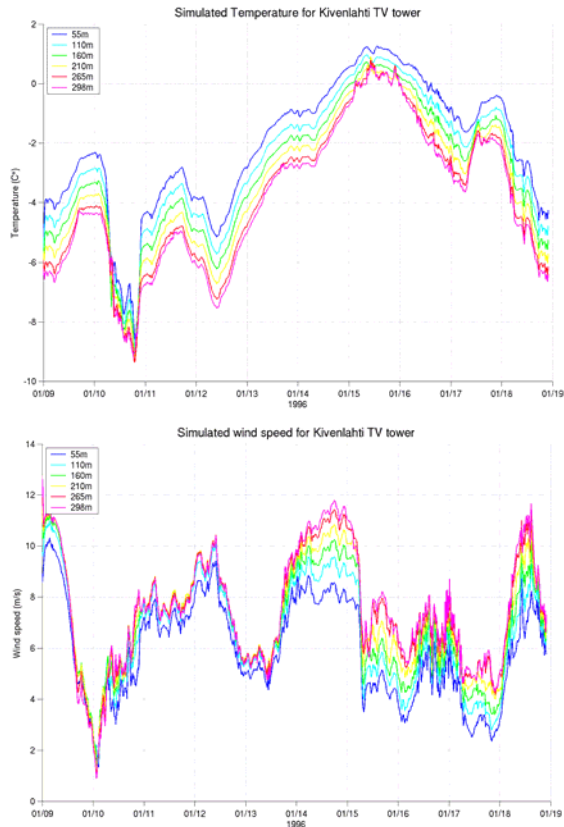


Fig. 4. Time-series of temperature ($^{\circ}\text{C}$; upper panel) and wind speed (m/s; lower panel) from the WRF simulation at the Kivenlahti TV tower. Each curve corresponds to a different vertical level in the model.

illustrative purposes, this error was compensated for in the calculations of ice load by assuming temperature did not rise above melting.

As expected, there are other discrepancies between model and observations as well, including intermittent periods of very light snow and/or drizzle found in the simulations, though the amount of simulated precipitation over ten days is quite small, 6 mm. Time-series plots of WRF cloud water and drizzle in Fig. 5 clearly indicate a nearly continuous period of clouds matching observations very well, even if the details of the liquid water amounts are not entirely known. Any periods in the model simulation with freezing drizzle produce a rapid ice growth since water drops of that size have a very high collection efficiency compared to the small cloud droplets. Using the LWC from both classes of water to calculate the ice accretion, as described in section 3, results in the ice loads shown in Fig. 6.

These simulated ice loads are roughly half of what was observed by the third author upon sampling the ice from the tower on 18 Jan, but we believe the case clearly illustrates the potential usefulness of the WRF simulations. The under-prediction of ice accretion is most likely due to simulated liquid water content of cloud water being lower than what was observed. Perhaps the simplistic approach of constant droplet number concentration, which directly affects the production of rain is responsible for a portion of the error. In this event, the pre-set number of drops was 100 cm^{-3} , whereas a larger value would cause a slight decrease in occurrence of rain and there-

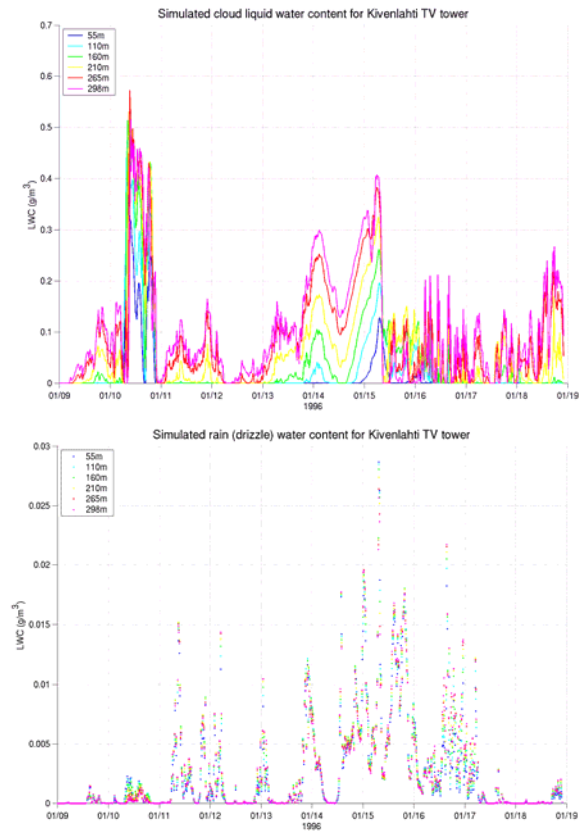


Fig. 5. As in Fig. 4 except cloud water content (cm^{-3} ; upper panel) and drizzle content (cm^{-3} ; lower panel).

fore allow cloud water to increase. A sensitivity study with a different value of cloud droplet concentration may be attempted in the future.

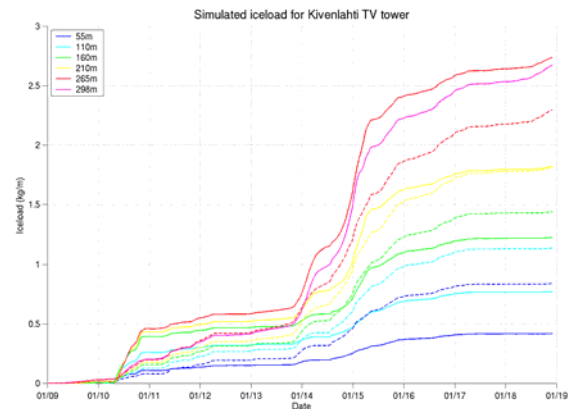


Fig. 6. As in Fig. 4 except ice load (kg m^{-1}).

B. Guetsch, Switzerland, 13-14 November 2008

The COST-727 icing test site at Guetsch in the Swiss Alps near Andermatt experienced a moderate to strong icing event on 13-14 Nov 2008. The site has measurements of icing using a Combitech and Rosemount icing detectors, though the latter malfunctioned during this event. The Combitech ice detector showed a bias during the observed icing period, but clearly captured some useful data as seen in Fig. 7. The most rapid build-up of ice occurs early on 13 Nov and continues for nearly

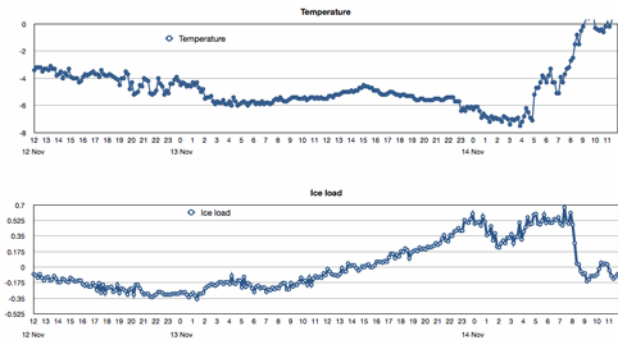


Fig. 7. Time-series plot of temperature and Combitech ice load at Guetsch, Switzerland.

24 h, then a period of intermittent icing in the first 8 h of 14 Nov before ending completely as the cloud cleared.

The WRF results of the case are shown in Fig. 8 and indicate a supercooled liquid water cloud appears in very low quantity during the day on the 12th. The model also had steady light snow falling, approximately 1 mm hr^{-1} , before the snow decreases and larger amounts of cloud water begin to form at approximately the correct time. Though the simulation was not completed for the 14th, WRF was trending to reduce clouds in the Alps as a strong storm system moved eastward along the southern side of the mountains and took most of the moisture away ahead of the observations. Most of the simulated liquid cloud dissipates as early as 9 h ahead of the observations. Ice load calculations will be carried out in future work and compared to available observations.

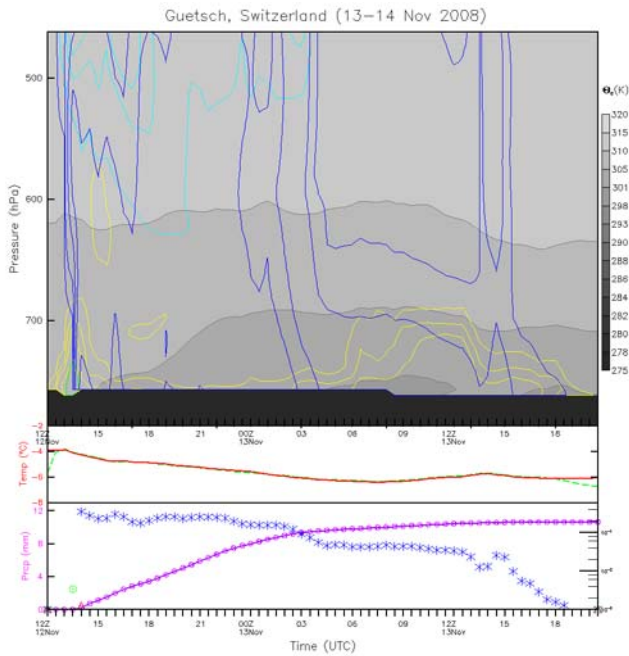


Fig. 8. Time-height diagram (upper panel) with Theta-E (K; gray shades), cloud ice content (cyan contours), snow content (blue contours), cloud water content (yellow contours); middle-panel: temperature (red) and dewpoint (green); lower-panel: precipitation reaching the surface (magenta), and hydrometeor type and amount at the surface for WRF model gridpoint nearest Guetsch, Switzerland.

C. Luosto Fell, Finland, Case1: 19-20 April 2006

The COST-727 icing test site at Luosto Fell in northern Finland experienced several icing events that were discussed in Hirvonen et al (2007). Though not in chronological order here, the cases are presented as in the reference and only limited subjective comparisons are made between WRF model results and the subjective icing classifications of Hirvonen. In this first case, the icing was characterized as light to moderate and intermittent light snow was observed. The upper panel of Fig. 9 shows the time-series plot of temperature, dewpoint, and

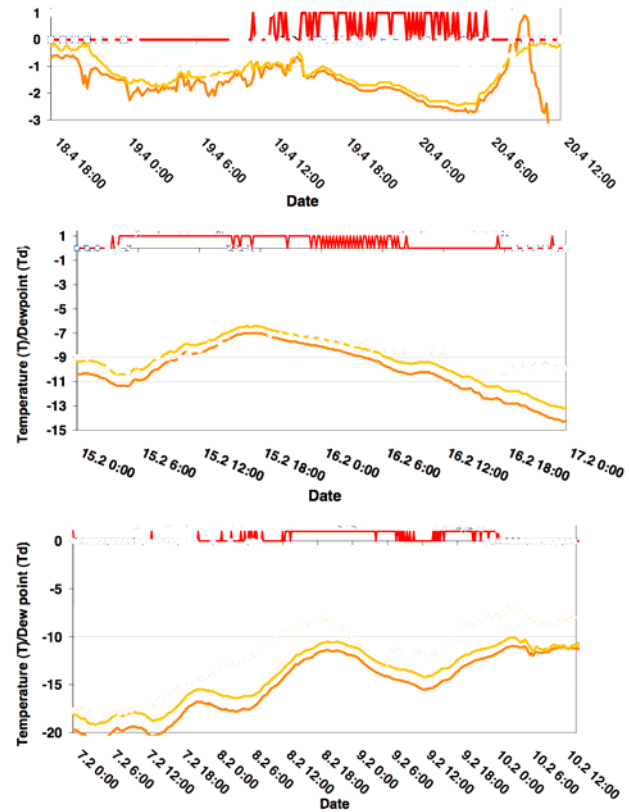


Fig. 9. Time-series plot of temperature and Rosemount icing probe at Luosto, Finland for the three cases.

Rosemount icing probe data (0 = no icing; 1 = icing). The event generally started around 1200 UTC 19 Feb and ended approximately 0600 UTC 20 Feb. In approximately 12 h of very light intermittent rain and snow showers, the site reported 2.4 mm of precipitation.

A time-height graphic created from the WRF simulation, shown in Fig. 10, reveals a supercooled liquid water cloud (yellow contours) was predicted by the model a few hours later and persisted a few hours longer than observed. The model also forecasted intermittent light snow (blue contours) accumulating nearly 3 mm in about 18 hours. The intermittent nature of the event and the overall low liquid water content suggests a reasonable match to the observations.

D. Luosto Fell, Finland, Case2: 15-16 February 2006

The same site experienced a much more impressive icing event a few months prior, which was characterized as continu-

ous and severe. The time-series of temperature, dewpoint, and icing data is shown in the middle panel of Fig. 9. Note the icing occurs during the entire day on the 15th and well into the first half of the 16th.

The WRF model did an excellent job with this case, probably because it included strong synoptic forcing and a shallow layer of cold air with a strong temperature inversion above the cloud. The time-height from model results is shown in Fig. 10

and indicates a long-lived, shallow, supercooled liquid water cloud in contact with the ground. Only a trace amount of precipitation (snow) is falling from the cloud. Cloud water amounts from the model for this case reach as high as 0.5 g m^{-3} .

E. Luosto Fell, Finland, Case3: 8-10 February 2006

The next case study from Luosto was less severe than case 2, but it was still classified as continuous and moderate to severe. The observed data are shown in the lowest panel of Fig. 9 and indicate the lowest temperatures of these three cases and an intermittent signal from the icing probe early on the 8th, followed by more continuous icing towards the latter half of the day and continuing most of the next day.

The WRF model results (not shown) of this case were less impressive with a complex double-layer cloud producing snow above a supercooled liquid water cloud near to, but not touching the surface. The predicted temperature matched observations quite well, but the liquid cloud was less continuous as some snow was falling from the upper cloud and depleting the liquid water of the low cloud. Nonetheless, the prediction of a liquid and mixed-phase cloud at temperatures below -15°C may be considered an achievement compared to operationally-available data only a few years prior. Most cloud physics schemes rapidly produce glaciated conditions, not liquid at these temperatures.

F. Appalachian Mountains, USA, 4-5 February 1998

This event was characterized by strong and deep synoptic-scale lift associated with a developing cyclone along the East Coast of the United States. Snow accumulations varied greatly with elevation in the Appalachian mountains from 15 cm at 180 m elevation to 40 cm reported near 360 m. Besides snow, there was a significant accumulation of ice that produced widespread damage to trees and power/phone lines including a report of 12 cm ice accumulation on Poor Mountain (vicinity of Roanoke, Virginia) and \$607,000 clean-up cost from debris/damage to trees within Shenandoah National Park (NCDC, 1998). The freezing rain and ice pellet conditions also extended westward into the Ohio River valley region and was sampled by a NASA Twin Otter aircraft.

At 1200 UTC 4 Feb 1998, a vigorous upper-level trough extended from Iowa to Georgia with an associated surface low-pressure system near the Georgia-South Carolina border. A broad region of surface high pressure and cold air was found over much of the upper Midwest and neighboring Canada. These conditions resulted in a strong pressure gradient across the eastern third of the United States producing strong, low-level winds blowing inland from the Atlantic Ocean. Deep ascending moisture was present from the Carolinas into Pennsylvania with some dry mid-level air to the north and west of the Appalachians causing snow to sublimate before reaching the ground in the northern third of Ohio and Pennsylvania.

West Virginia and portions of adjacent states were at the center of a classic ice pellet and mixed rain/snow event with precipitation falling through a shallow melting layer, followed by sub- 0°C temperatures near the surface. The northwest portion of the surface precipitation shield primarily consisted of snow while the southeast portion contained rain throughout the

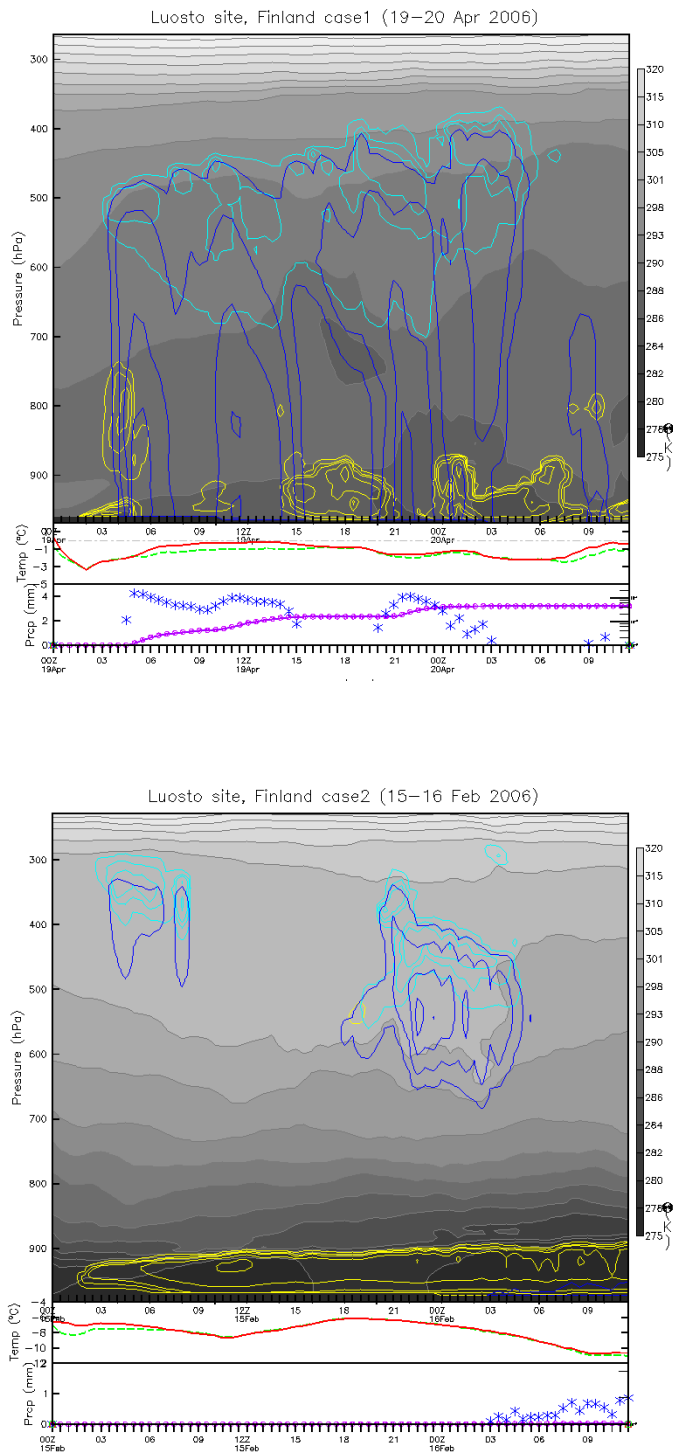


Fig. 10. As in Fig. 8 except for simulation of Luosto, Finland, Case 1 (upper panel), and Case 2 (lower panel).

event. A zone in between contained mixed conditions of snow with rain, snow or rain with ice pellets, and a few spotty locations of freezing rain. This general pattern persisted during the day with a gradual movement north and west as the melting layer was advected farther inland while the surface low-pressure moved slowly northward along the coast.

The NASA Twin Otter departed KCLE at 1430 UTC and searched for potential pockets of icing above the highest freezing level between there and Columbus, Ohio, but only snow and very little liquid were found. The aircraft then descended into and examined the freezing rain layer below 1220 m over southeast Ohio to the northwest of Parkersburg, West Virginia (KPKB) around 1600–1700 UTC. After sampling cloud and precipitation properties and landing at KPKB, a second flight commenced from 1800 to 2000 UTC in which NNW-SSE transects were flown at 915 m over KPKB. On this flight, bumpy glaze ice accreted on the aircraft (including 2.5 cm tall ridges aft of the deicing boots) resulting in a significant performance degradation (Bernstein et al., 1999). After landing at KPKB a second time, the aircraft ferried back to KCLE between 2200 and 2355 UTC.

The Twin Otter spent most of the time from 1630 to 2230 UTC in the vicinity of KPKB. During this time, the aircraft sampled the cloud and precipitation features above, within, and below a melting layer found between 1200 and 2100 m, which had a maximum temperature of 2°C. Below this melting layer was a subfreezing layer with minimum temperature of -2.8°C while the surface temperature was nearly 1°C, hence a second melting layer existed in contact with the surface. METAR observations from KPKB (as well as Twin Otter crew members) indicated rain, ice pellets, and/or snow grains from 1648 to 1850 UTC. Aircraft data from 1817–1824 UTC revealed snow throughout the sampling

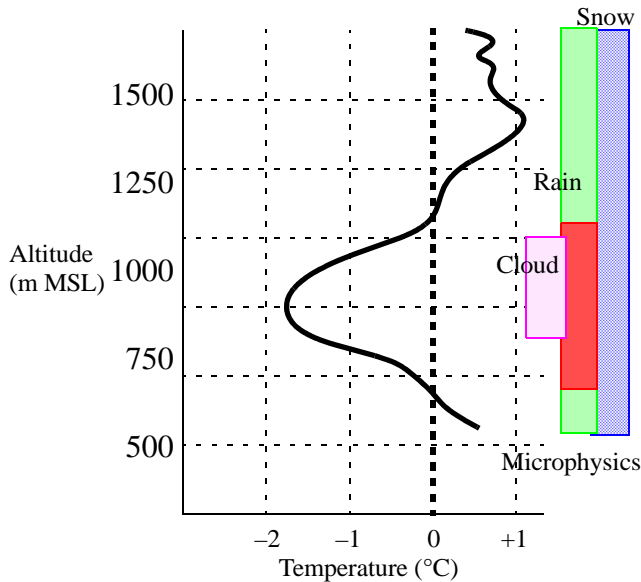


Fig. 11. Temperature (°C) and microphysics encountered by the NASA Twin Otter while sampling near Parkersburg, WV between 1817 and 1824 UTC 4 Feb 1998. The red dot-filled box represents freezing rain conditions.

region including below and within the melting layer. Rain, created by melted snow, was found there as well, which became freezing rain within the sub-0°C layer below approximately 1200 m. Cloud liquid water was also found between 640 and 1000 m (see Fig. 11). This basic structure was quite persistent throughout the entire sampling period with a reduction in snow found within/below the melting layer toward the end of the period as warmer air infiltrated from east to west.

The WRF simulation results successfully reproduced all of the primary structures of the case including the multiple freezing levels, snow mixed with rain and freezing rain, and even the prediction of ice pellets (graupel in the model). A north-to-south cross-section showing all the microphysics species is found in Fig. 12 and shows a troposphere-deep ice and snow cloud falling down to the melting level where rain forms, but, depending on the depth of air warmer or colder than melting temperature, different precipitation results. Where the warm layer is extremely shallow, the snow melts to produce a minimal amount of rain, but then this rain quickly re-freezes into graupel (equivalent to ice pellets since those are not explicitly treated in this microphysics scheme). Where the melting layer is slightly deeper, the snow either partially or fully melts to form rain that subsequently falls into a sub-0°C layer to make freezing rain. And, finally, further south, the melting layer is in contact with the surface and the snow simply melts to rain, which falls as such to the ground.

VI. SUMMARY AND CONCLUSIONS

In general, the WRF model shows skill to predict events of ground/structural icing. In cases of deep and widespread synoptic or mesoscale lift, the model is more dependable than events with small-scale and/or weak lifting. While the timing of some events and the specific forecast of liquid water content will not be perfect, the model is capable of providing estimates of start and end times of various ground icing events as well as

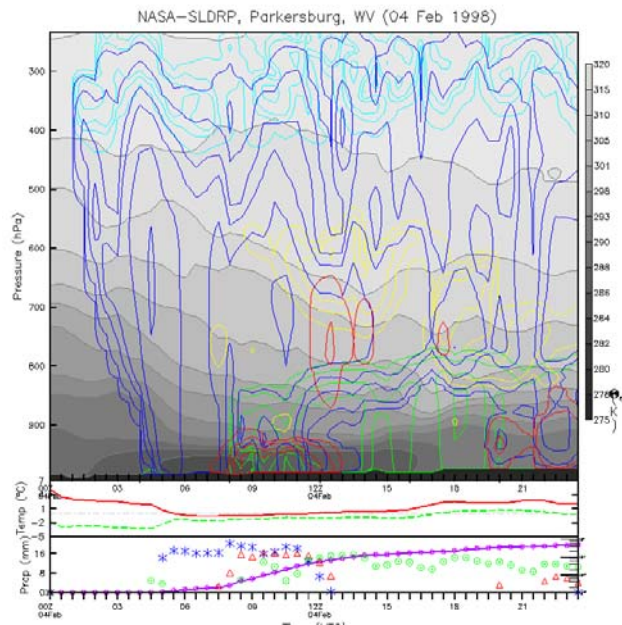


Fig. 12. As in Fig. 8 except for simulation of Parkersburg, WV, (subsection F).

some usefulness for predicting icing growth, even if those are subjective estimates of light, moderate, and severe icing. As data assimilation techniques improve and more complex physics are included in a model, as well as faster computers allow finer-scale resolutions, the simulations of explicit ground/structural icing will likely improve further in future decades.

VII. ACKNOWLEDGEMENTS

The authors wish to thank Ben Bernstein for providing details of the 4 Feb 1998 case and Roy Rasmussen and Marcia Politovich for many fruitful cloud physics discussions. Also, the members of the COST-727 icing teams are gratefully acknowledged for their diligent work to create and maintain a valuable network of ground icing measurement sites.

VIII. REFERENCES

- Bernstein, B. C., T. P. Ratvasky, D. R. Miller, and F. McDonough, 1999: Freezing rain as an in-flight hazard. *Preprints, 8th Conference on Aviation, Range, and Aerospace Meteorology*, Dallas, TX, Amer. Meteor. Soc., 38–42.
- Makkonen, L., 2000: Models for the growth of rime, glaze, icicles and wet snow on structures. *Phil. Trans. R. Soc. London*, **358**, 2913–2939.
- NCDC, 1998: http://www4.ncdc.noaa.gov/cgi-win/wwcgi.dll?wwEvent_storms
- Skamarock, W. C., J. B. Klemp, J. Dudhia, D. O. Gill, D. M. Barker, M. Duda, H. Huang, W. Wang, and J. G. Powers, 2008: A description of the advanced research WRF version 3. NCAR Tech. Note NCAR/TN-475+STR, 113 pp.
- Thompson, G., R. M. Rasmussen, and K. Manning, 2004: Explicit forecasts of winter precipitation using an improved bulk microphysics scheme. Part II: Implementation of a new snow parameterization. *Mon. Wea. Rev.*, **136**, 5095–5115.